Morphological Profile of Atypical Femoral Fractures: Age-Related Changes of the Cross-sectional Geometry of the Diaphysis

Takeshi Imamura[1]
Toshiyuki Tsurumoto[1] *
Kazunobu Saiki [1]
Keita Nishi[2]
Keishi Okamoto[1]
Yoshitaka Manabe[2]
Joichi Oyamada[2]
Keiko Ogami-Takamura[1]

[1]Department of Macroscopic Anatomy, Graduate School of Biomedical Science, Nagasaki University, Nagasaki 852-8523, Japan
[2]Department of Oral Anatomy and Dental Anthropology, Graduate School of Biomedical Science, Nagasaki University, Nagasaki 852-8523, Japan
*corresponding author; tsurumot@nagasaki-u.ac.jp

Short running page heading;
Cross-sectional Geometry of Femoral Diaphysis

Abstract

The use of bisphosphonates for osteoporosis patients has markedly decreased the incidences of femoral neck or trochanteric fractures. However, anti-osteoporosis drugs have been reported to increase the incidence of atypical femoral fractures (ATFFs), which involve stress fractures in the subtrochanteric region or the proximal diaphysis. In this study, the morphological characteristics of the cortical bone in human femoral diaphysis samples were analyzed from individuals who lived before bisphosphonate drugs were available in Japan. A total of 90 right femoral bones were arbitrarily selected (46 males and 44 females) from modern Japanese skeletal specimens. Full-length images of these femurs were acquired using a clinical CT scanner, and the data were saved in Digital Imaging and Communication in Medicine (DICOM) format. An image processing method for binarization was used to calculate the threshold values of individual bones for determining their contours. The range between the lower end of the lesser trochanter and the adductor tubercle of each femur was divided at regular intervals to obtain 10 planes. The area of cortical bone to the total area of cross-section (ACS) of the femoral mid-diaphysis was calculated as the cortical index at Level 5 (CI_5). Moreover, the mean value of cortical bone thickness (mCBT), periosteal border length (PBL), and ACS were evaluated for all planes. A comparison between males and females demonstrated that most females had lower CI_5 values than males. The femoral outer shape did not differ markedly according to age or sex; however, substantial individual differences were

observed in the shape of the inner surface of the cortical bone. Both mCBT and ACS decreased with age in the femoral diaphysis; however, in females, the reduction rate was higher for mCBT than for ACS. This may be due to a compensatory increase in the circumference of the femoral diaphysis. In addition, about half of the subjects had a small gap between the region with maximal mCBT and that with maximal ACS in the femoral shaft. Biological responses to mechanical stresses to the femoral diaphysis were not uniform. Bisphosphonate inhibit bone resorption, and may promote non-physiological bone remodeling. Thus, a nonhomogeneous decrease in cortical thickness may be related to the fracture=occurrence in the femoral diaphysis in some cases. Thus, long-term administration of bisphosphonates in patients with morphological vulnerability in the femoral cortical bones may increase the occurrence of ATFF.

1. Introduction

Osteoporosis is an age-related degenerative disease associated with fractures of the limb bones or spine, which markedly reduces the quality-of-life of elderly patients (Kanemaru et al., 2010; Abimanyi-Ochom et al., 2015). Accordingly, osteoporosis drugs, such as bisphosphonates, are administered to increase bone density not only in the lumbar spine but also in the proximal femur (Bone et al., 2004). In addition, reports have shown that some of these drugs reduced the incidences of femoral neck or trochanteric fractures (McClung et al., 2001; Papapoulos et al., 2005). However, osteoporosis drugs may increase the incidence of atypical femoral fractures (ATFFs), such as stress fractures, in the subtrochanteric region or the proximal diaphysis. In particular, bisphosphonate formulations have been associated with such fractures (Shane et al., 2010; Shane et al., 2014; Schilcher et al., 2015). In addition, some reports have suggested that the morphology of the proximal femur or the shape of the cortical bone is involved in the anatomical background of ATFFs (Koeppen et al., 2012; Hagen et al., 2014; Taormina et al., 2014; Niimi et al., 2015; Szolomayer et al., 2017). Bilateral femoral stress fractures in patients not taking a bisphosphonate drug have been reported (Donnelly et al., 2012). Therefore, femoral morphological characteristics may be responsible for the occurrence of these fractures.

As micro-computed tomography (CT) and various morphological analyses are increasingly being used, more discoveries on the structural analysis of cancellous bone have been reported (Burr, 2010; Geissler et al., 2015). Because osteoporosis drugs with various mechanisms of action have become available, cortical bone is attracting attention as a target for fracture prevention (Mizushima et al., 2009). Thus, a morphological review of the long bones, especially the bone shape of the femoral diaphysis, is necessary. Marcauo et al. (2014) found that Asians are at high risk of atypical bisphosphonate-associated fractures. Sex differences in the cross-sectional morphologies of human long bones with aging were reported in native Americans (Ruff et al., 1983) and in blacks and whites (Schlecht et al., 2015; Japsen et al., 2015). To clarify the background of ATFFs, the morphological characteristics of cortical bone in the human femoral diaphysis were analyzed in Japanese individuals who lived before bisphosphonate drugs were developed.

In quantitative evaluations using CT images, the method for calculating the contour threshold should be strictly defined. This study used the mode method, an image processing method for calculation of the threshold. This binary method is useful when the histogram of values shows a bimodal distribution in CT images (Chow et al., 1972; Bousson et al., 2004; Chen et al., 2010). Using the method, a single threshold was determined for each individual, and the contour of the cortical bone was strictly determined. A new method to measure cortical bone thickness (CBT) was used to perform a quantitative analysis of the cortical bone of the femoral diaphysis.

2. Materials and Methods

2.1. Materials

Among skeletal specimens from modern Japanese stored at Nagasaki University, 90 right femurs, including 46 from males aged 20–89 years (mean age, 62.7 years) and 44 from females aged 31–87 years (mean age, 68.3 years), were included in the study. They were obtained from cadavers provided to the Nagasaki University School of Medicine for anatomical dissection by medical students between the 1950s and 1970s. Most of them were voluntarily donated, and most were from anonymous subjects. The sex and exact ages at death of all the individuals were registered. After their dissection, their soft tissues were almost entirely removed to produce dry skeletal preparations. Those with obvious trauma or inflammatory joint diseases were excluded. Because their year of death was approximately between the 1960s and 1970s, none of the subjects could have possibly taken bisphosphonate drugs before their deaths. Before being further divided according to sex, the subjects were divided into two groups by age as follows: group A (≤69 years old; 30 males and 16 females) and group B (≥70 years old; 16 males and 28 females).

2.2. CT imaging and extraction of the target images

Full-length images of all the examined femurs were obtained using clinical multislice CT (Activision 16, Toshiba Corp. Japan) (X-tube volume/current = 120 kV/100 mA, Image matrix size; 512 × 512 pixels, slice thickness; 0.5 mm). The bones were placed in a natural position with the posterior side down on the table of the imaging device. CT images of the femurs were obtained after the regions of interest were adjusted to maximize the images, which meant that the field of view (FOV) was approximately 100 mm × 100 mm. The data were saved in Digital Imaging and Communication in Medicine (DICOM) format.

The range between the lower end of the lesser trochanter and the adductor tubercle of each femur was divided into nine segments of equal length. Then, all of the cross-sections, including both ends, were labeled from top to bottom as "Level 1" to "Level 10". Namely, Level 1 was the section at the lower end of the lesser trochanter, and Level 10 was the section of the tip of adductor tubercle. Segmenting was performed using a Microsoft VBA formula with CT image numbers that were assigned automatically by the CT equipment. These selected ten sections were subjected to the following processes.

2.3. Determination of the threshold and the principle of contour extraction

Each of these obtained DICOM data files was opened with ImageJ ver. 1.50 (NIH, USA) and saved as a text image file. A 512 × 512 matrix consisting of text data of CT values was obtained. This text file was then opened in Microsoft Excel (Office 2016, 64-bit, Microsoft Corporation, USA) and converted to an xls file. Based on these values, the threshold for determining each femoral contour was determined as follows: (i) all of the matrixes for these ten sections were pasted into one Microsoft Excel sheet; and (ii) a histogram was created based a frequency table of CT values to calculate the mean CT value for the first peak (i.e., approximately -1,000; mainly indicating the CT value of the surrounding air) and the CT value for the second peak (i.e., indicating the CT value of the bone itself). This value was used as a threshold to determine the cortical bone contour of the target bone (Figure 1). This is a unique value for each individual. The endosteal and periosteal contours of the cortical bone were determined using a single threshold in all the slices for each individual.

2.4. Study items

Out of the ten area of cross-section (ACS) evaluations, seven ACS values at Levels 2–8 showing the shape of the diaphysis were selected. The following steps were applied to calculate each value for each ACS. In addition, the 512 × 512 matrix of the CT values from each cross- section was opened with Microsoft Excel (Office 2016, 64-bit), and the following calculations and image processing were performed using Microsoft Excel functions and Visual Basic for Applications (VBA). In this analysis, all foramina (openings or holes) in the segmented cortical bone region without continuity with the bone marrow cavity were regarded as cortical bone regions and analyzed further as follows.

i) Cortical index at the femoral mid-diaphysis level

The ratio of the area of the cortical bone to the total ACS of the femoral mid-diaphysis at Level 5 (i.e., the occupancy rate of the cortical bone) was calculated as the cortical index at Level 5 (CI_5; Figure 2, right, b / [b + c] × 100).

ii) Mean cortical bone thickness

Distances between a point on the periosteal surface and all points on the endosteal surface of the cortical bone were calculated. The minimum of these values was defined as the CBT of the point. Such calculations were performed for all points of the periosteal surface of the cortical bone to calculate the CBT of the entire circumference of the cortical bone (Figure 2, left). All of the CBT in one cross-section were then averaged to obtain a mean value for CBT (mCBT).

iii) Area of cross-section

The ACS of each section was calculated by counting all points (pixels) in the area surrounded by the periosteal and endosteal perimeters of the cortical bone (Figure 2, right). b). The area was corrected by calculating the actual length per pixel in the DICOM data to take into account the magnification ratio at the time of imaging.

iv) Periosteal border length

The periosteal border length (PBL) of each section was calculated by counting the number of all points (pixels) on the periosteal surface using Microsoft Excel (Figure 2, left, a).

2.5. Statistical analysis

Pearson correlations were performed to test the relationship between mCBT, PBL, ACS, and CI_5 for each slice location and age. Differences in mCBT, PBL, ACS, and CI_5 between the two age groups at each cross-sectional position along the diaphysis were assessed using Student's *t*-test.

3. Results

3.1. Example presentation

The analysis results for a 70-year-old female and a 60-year-old female are shown in Figures 3 and 4. In Figure 3, the degree of CBT is visualized using conditional formatting in Microsoft Excel; the thicker the cortex, the deeper the red, whereas the thinner the cortex, the deeper the blue. In Figure 4, the shape of the cross-sections for the seven levels is visualized. The values of mCBT (mean ± standard deviation), PBL, and ACS are shown in the table. Progression of osteoporosis was observed in the 70-year-old female.

3.2. Morphological analysis of the section at Level 5

In Figure 5, the cross-sectional images at Level 5 for each individual are shown in ascending order of CI values. Respective scale factors are not the same to determine the shape and proportion. In addition, all foramina in the cortical bone region are shown as cortical bone regions. Blue indicates males, and red indicates females. The comparison between the males and females demonstrated that most females had lower CI values than males. Regardless of the CI value, the apparent linea aspera tended to remain unchanged. However, in individuals with lower CI values, the part of the cortical bone corresponding to the linea aspera was thinner on the linea aspera side. Furthermore, in individuals with higher CI values, the cortical bone became thicker at the three following places: the posterior part where the linea aspera is located, the inner part, and the outer part.

CI_5 was calculated by extracting the shape of the ACS at Level 5 (i.e., the femoral mid-diaphysis) in all 90 individuals. Figure 6-a is a scatter plot showing the relationship between CI_5 and the age of each individual according to sex. This showed a negative correlation in females ($r = -0.60$). CI decreased with age but without statistical significance ($r = -0.28$) in males.

Figure 6-b shows box plots of the CI_5 values according to age (i.e., group A, ≤69 years old and group B, ≥70 years old) and sex. Females showed a significant difference between these two groups.

For the section at Level 5, there was a significant positive correlation between the ACS and PBL ($r = 0.74$ in males, 0.43 in females); however, the correlative coefficient between mCBT and PBL was relatively low ($r = 0.23$ in males, 0.07 in females). This meant that PBL affected the value of ASC more than mCBT.

3.3. Measurements of mean cortical bone thickness

Figure 7-a shows box plots of mCBT values at Levels 2–8 according to age (i.e., groups A and B) and sex. The average mCBT had a maximal value at Level 4 (i.e., a section slightly

proximal to the femoral mid-diaphysis) in all the groups. The overall mCBTs in males was higher than those in females. In females with lower mCBT values for all the sections, their mCBTs at around Levels 2–5 showed an almost flat curve. A comparison between groups A and B found significant differences at Levels 7 and 8 (i.e., the distal part) in males. In contrast, the CBT in group A was significantly greater than that in group B in all sections except Level 2 in females.

Figure 7-b is a scatter plot showing the relationship between average mCBT values and age in males and females. In females, mCBT decreased significantly with age ($r = -0.53$). In males, the mCBT decreased with age but without statistical significance ($r = -0.22$).

3.4. Measurement of the area of cross section

Figure 8-a shows box plots of the ACS values at Levels 2–8 according to age (i.e., groups A and B) and sex. Comparison of the measurement results according to Level and sex showed higher values in males compared with females. As with mCBT, the mid-diaphysis had higher ACS values. The ACS curves for all the groups were relatively flatter than the mCBT curves (Figure 8-a). When individual ACS values were examined, some females with lower ACS average values for all the sections had flat curves in the mid-diaphysis. The comparison between groups A and B according to sex showed that in females, group A had higher ACS values at Levels 5–8 than group B.

Figure 8-b is a scatter plot showing the relationship between ACS values and age in males and females. ACS in males showed almost no decrease with age (r = -0.12), whereas a significant negative correlation was observed in females (r = -0.33).

3.5. Measurement of periosteal border length

Figure 9-a shows box plots of the PBL values at Levels 2–8 according to age (i.e., groups A and B) and sex. Both males and females showed similar curves for Levels 2–6 (i.e., a range between a section slightly below the lower end of the lesser trochanter and a section slightly distal to the mid-diaphysis). However, the PBL for a range between a section slightly below the lower end of the lesser trochanter and the mid-diaphysis tended to decrease slightly in females. Some males also showed a similar tendency. The comparison between groups A and B according to sex showed that group B had significantly higher PBLs at Levels 2, 4, 5, and 6 than group A in males.

Figure 9-b is a scatter plot showing the relationship between average PBL values and age for each individual according to sex. The correlation between the PBL values and age of each individual showed that PBL increased with age (r = 0.30) in females. Namely, the circumference of the femur increased significantly with age in that group of patients.

3.6. Comparison between the level of the maximal mCBT and that of the maximal ACS

The level of the maximal ACS value and that of maximal mCBT in each femoral bone is shown in Table 1. The mCBT values were principally maximal at Levels 3 or 4. On the other hand, the ACS values were maximal at Levels 2 or 3. In 48 of 90 individuals, the region with the largest ACS was located more proximal to the region with the largest mCBT.

4. Discussion

4.1. Method for determining the contour of the cortical bone using CT images

The CT values of the measured objects obtained using a medical CT (Hounsfield units [HUs]) are proportional to the X-ray linear attenuation coefficients of the objects. Measurements were performed on data extracted from the DICOM file image format that was generated using the clinical CT scanner. To measure the shape of the object based on such CT image data, it is necessary to determine the contour of the object accurately. The appropriate CT value has been commonly used as a threshold after setting the regions of interest for each cross-section image and determine the contour based on the threshold. However, the contour of an object due to the partial volume effect is difficult to determine accurately (Ward et al., 2005; Scherf et al., 2009). Therefore, if the method used to determine the threshold is unclear, the size of the object cannot be measured accurately. The half-maximum height thresholding protocol (Coleman et al., 2007; Kazakia et al., 2014) adaptive interactive thresholding method (Leung et al., 1996;

Ryan et al., 2002) of bone and background showed a clear bimodal distribution in this study. The mode method, an image processing method for binarization, can be used to determine the contour of bone (Chow et al., 1972; Bousson et al., 2004; Chen et al., 2010). This study applied the mode method to determine the contour of bone using CT values for the first and second peaks in the histogram on images obtained from DICOM data as the threshold for each individual.

4.2. Changes in the shape of the human femoral diaphysis with aging

In vertebrates with an endoskeleton, bone tissue repeats bone formation and bone resorption throughout life. During these processes, various changes occur in the morphology of the bone marrow cavity and cortical bone. Several cross-sectional studies evaluating age differences in humans have been conducted (Smith et al., 1964; Ruff et al., 1982; MacIntosh et al., 2013). The femoral diaphysis continues to grow even after adulthood. A functionally adaptive increase in the contour length of the femoral diaphysis to compensate for osteoporotic reduction in bone strength may be one of the reasons for the changes in the morphology of the diaphysis over time. However, an age-related increase in the contour length of the femoral diaphysis was not observed in males and females (Shibata, 1992). As shown in Figure 9, we found that PBL increased gradually with age in males and females. However, CBT decreased significantly with age, especially in females. This may be due to expansion of the bone marrow cavity by trabecularization of the cortical bone (Ostertag et al., 2014).

Women have less cortical area than expected for their body size and bone size, which in part explains their reduced bone strength compared with the more robust bones of men (Japsen et al., 2015; Schlecht et al., 2015). Our study, in which the femoral bones of middle-aged and older individuals were analyzed, showed differences in the cross-sectional morphology of the femoral diaphysis between males and females, and the sex distinction was significant in older individuals.

As shown in Figure 9, the femoral outer shape did not differ markedly according to age or sex. Substantial individual differences were nevertheless observed in the shape of the inner surface of the cortical bone. Elderly females, in whom a rapid remodeling from cortical bone to cancellous bone occurred, were found to go through considerable changes that could not be inferred from the external bone appearance. Even among those whose linea aspera on the posterior surface of the femoral bone did not show apparent changes, the bone marrow cavity size of some individuals increased markedly due to the gradual trabecularization and cortical bone porosity.

4.3. Anatomical background of ATFF occurrence

Bisphosphonate drugs have become widely used as therapeutic agents for patients with osteoporosis, and cases of stress fractures (i.e., atypical subtrochanteric femoral or atypical fractures of the diaphysis), which rarely occurred in the past, are being reported more frequently. Indeed, a higher incidence of ATFF in patients with osteoporosis treated with bisphosphonates has been reported (Schilcher et al., 2011; Schilcher et al., 2015). Moreover, some morphological characteristics of cortical bones of the femoral diaphysis may influence the occurrence of ATFF (Koeppen et al., 2012; Hagen et al., 2014; Niimi et al., 2015; Szolomayer et al., 2017). However, the mechanisms involved are still unknown.

In this study, we examined morphological changes with ageing in cortical bones of the femoral diaphysis. First, the values of mCBT near the mid-diaphysis were larger in younger individuals. Moreover, thinning of the cortical bones progressed throughout the entire femoral shafts with ageing. Intra-individual regional differences in ACS values were smaller than those of mCBT, especially in females. We found that PBL values affected ASC values more than mCBT, which might be due to age-related expansion in the medullary cavities of the femoral diaphysis. Second, mCBT values were maximal at Levels 3 or 4 (i.e., a region slightly above the mid-diaphysis) in males and females. On the other hand, ACS values were maximal at a region slightly distal to the subtrochanteric region. Indeed, in more than half of the individuals, the region with the largest ACS was located more proximal to the region with the largest mCBT. That is, there were many individuals who had discrepancies between the regions with maximal mCBT and ACS values.

The morphological characteristics of bones change gradually via remodeling in accordance with Wolff's law. Our results suggested that biological responses to mechanical stresses to the femoral diaphysis are not uniform. Even so, almost all of these results were physiological phenomena. In contrast, bisphosphonates, which have different degrees of bone-resorption inhibiting effects, may promote non-physiological bone remodeling. In particular, the subtrochanteric region of the femoral shaft, which is a region of many muscle insertions, receives traction forces in various directions as part of activities of daily living. Additionally, mechanical stress is reported to be high in these regions if femoral shaft bowing was severe (Oh et al., 2014; Shin et al., 2017). The risk of the breakdown of the bone structure in advanced osteoporotic femoral diaphysis may increase with these various composite factors.

Fracture incidence is increased in various bones with aging in humans. It is speculated that not only morphological changes in bone but also qualitative changes, such as changes in the bone quality of cancellous and cortical bones, are involved. Patton et al. (2018) examined the relationships among age, sex, strength, and stiffness in both the femoral neck and femoral diaphysis, and found that a nonhomogeneous decrease in cortical thickness may be related to the high fracture incidence in the femoral diaphysis in some cases. Considering these results, when an individual with a morphological vulnerability in the femoral cortical bones takes long-term bisphosphonate, the risk of occurrence of ATFF may increase.

4.4. Limitations of this study

This study had some limitations: 1st) All the samples used in this study were femurs without actual atypical fractures. 2nd) This was a cross-sectional study of right femurs from 90 individuals. Thus, it was not possible to track morphological changes over time. 3rd) Records of health status, medication, and activities before death for each individual were not available. 4th) Due to the nature of the anatomical skeletal collection comprising a donor population, the sample was also skewed towards older age ranges. 5th) In addition, due to the nature of the samples, it was impossible to explore associations between diaphyseal morphology and mechanical properties.

5. Conclusions

In human femoral diaphysis, CBT and ACS decreased with age. This trend was particularly notable in females. However, a higher reduction rate in CBT than that in ACS was also observed in females. This may be partly due to an increase in the circumference of the femoral diaphysis compensating for a decrease in ACS. In addition, the results also showed that half of the individuals had discrepancies between the regions with maximal mCBT and those with maximal ACS values in the femoral shaft. Many muscle tendons are attached to these regions, which receive traction forces in various directions during activities of daily living. In these biomechanical circumstances in osteoporotic individuals, some degree of fragility may appear in the femoral bone. As an additional study, femoral bones of patients with ATFF should be analyzed to clarify their morphological characteristics using the methods adopted in this study.

Conflicts of Interest

The authors declare that there is no conflict of interest regarding the publication of this article.

Ethical approval

All procedures performed in this study were in accordance with ethical standards of the Ethics Committee of Nagasaki University Graduate School of Biomedical Sciences (approval number: 15033076) and with the 1964 Helsinki Declaration and its later amendments or comparable ethical standards.

References

Abimanyi-Ochom J, Watts JJ, Borgström F, et al. (2015) Changes in quality of life associated with fragility fractures: Australian arm of the International Cost and Utility Related to Osteoporotic Fractures Study (AusICUROS), *Osteoporosis International* 26, 1781–1790.

Bone GH, Hosking D, Devogelaer JP, et al. (2004) Ten years' experience with alendronate for osteoporosis in postmenopausal women, *N Engl J Med* 350, 1189–1199.

Bousson V, Peyrin F, Bergot C, et al. (2004) Cortical bone in the human femoral neck: Three-dimensional appearance and porosity using synchrotron radiation, *Bone Miner Res* 19, 794–801.

Burr DB (2010) Cortical bone: a target for fracture prevention? *Lancet* 375,1672–1673.

Chen H, Zhou X, Shoumura S, et al. (2010) Age- and gender-dependent changes in three-dimensional microstructure of cortical and trabecular bone at the human femoral neck, *Osteoporos Int* 21, 627–636.

Chow CK, Kaneko T (1972) Automatic Boundary Detection of the Left Ventricle from Cineangiograms, *Comput Biomed Res* 5, 388–410.

Coleman MN, Colbert MW (2007) Technical note: CT thresholding protocols for taking measurements on three-dimensional models, *Am J Phys Anthropol* 133, 723–725

Donnelly E, Meredith DS, Nguyen JT, et al. (2012) Reduced cortical bone compositional heterogeneity with bisphosphonate treatment in postmenopausal women with intertrochanteric and subtrochanteric fractures, *J Bone Miner Res* 27, 672–678.

Geissler JR, Bajaj D, Fritton JC (2015) Cortical bone tissue mechanical quality and biological mechanisms possibly underlying atypical fractures *J Biomech* 48, 883–894.

Hagen JE, Miller AN, Ott SM, et al. (2014) Association of atypical femoral fractures with bisphosphonate use by patients with varus hip geometry, *J Bone Joint Surg Am* 96, 1905–1909.

Jepsen KJ, Bigelow EM, Schlecht SH. (2015) Women Build Long Bones With Less Cortical Mass Relative to Body Size and Bone Size Compared With Men, *Clin Orthop Relat Res* 473, 2530–2539.

Kanemaru A, Arahata K, Ohta T, et al. (2010) The efficacy of home-based muscle training for the elderly osteoporotic women: The effects of daily muscle training on quality of life (QoL), *Arch Gerontol Geriatr* 51, 169–172.

Kazakia GJ, Tjong W, Nirody JA, et al. (2014) The influence of disuse on bone microstructure and mechanics assessed by HR-pQCT, *Bone* 63, 132–140.

Koeppen VA, Schilcher J, Aspenberg P (2012) Atypical fractures do not have a thicker cortex, *Osteoporos Int* 23, 2893–2896.

Leung CK, Lam FK (1996) Performance Analysis for a Class of Iterative Image Thresholding Algorithm, *Pattern Recognition* 29, 1523–1530.

MacIntosh AA, Davies TG, Ryan TM, et al. (2013) Periosteal versus true cross-sectional geometry: A comparison along humeral, femoral, and tibial diaphyses, *Am J Phys Anthropol* 150, 442–452.

Marcano A, Taormina D, Egol KA, et al. (2014) Are race and sex associated with the occurrence of atypical femoral fractures?, *Clin Orthop Relat Res* 472, 1020–1027.

McClung MR, Geusens P, Miller PD, et al. (2001) Effect of risedronate on the risk of hip fracture in elderly women, *N Engl J Med* 344, 333–340.

Mizushima S, Sakaue K (2009) Age-Related Changes in the External and Midshaft Cross-Sectional Geometries of the Adult Recent Japanese Femur, *Anthropol Sci Japanese Series* 117, 99–110.

Niimi R, Kono T, Nishihara A, et al. (2015) Cortical thickness of the femur and long-term bisphosphonate use, *J Bone Miner Res* 30, 225–231.

Oh Y, Wakabayashi Y, Kurosa Y, et al. (2014) Potential pathogenic mechanism for stress fractures of the bowed femoral shaft in the elderly: Mechanical analysis by the CT-based finite element method, *Injury* 45, 1764–1771.

Ostertag A, Peyrin F, Fernandez S, et al. (2014) Cortical measurements of the tibia from high resolution peripheral quantitative computed tomography images: A comparison with synchrotron radiation micro-computed tomography, *Bone* 63, 7–14.

Papapoulos SE, Quandt SA, Liberman UA, et al. (2005) Meta-analysis of the efficacy of alendronate for the prevention of hip fractures in postmenopausal women, *Osteoporos Int* 16, 468–474.

Patton DM, Bigelow EMR, Schlecht SH. (2018) The relationship between whole bone stiffness and strength is age and sex dependent, *J Biomech* 83, 125–133.

Ruff CB, Hayes WC (1983) Cross-sectional geometry of Pecos Pueblo femora and tibiae - A biomechanical investigation: I. Method and general patterns of variation, *Am J Phys Anthropol* 60, 359–381.

Ruff CN, Hayes W (1982) Subperiosteal expansion and cortical remodeling of the human femur and tibia with aging, *Science* 217, 945–948.

Ryan TM, Ketcham RA (2002) Femoral head trabecular bone structure in two omomyid primates, *J Hum Evol* 43, 241–263.

Scherf H, Tilgner R (2009) A new high-resolution computed tomography (CT) segmentation method for trabecular bone architectural analysis, *Am J Phys Anthropol* 140, 39–51.

Schilcher J, Howe TS, Png MA, et al. (2015) Atypical Fractures are Mainly Subtrochanteric in Singapore and Diaphyseal in Sweden: A Cross-Sectional Study, *J Bone Miner Res* 30, 2127–2132.

Schlecht SH, Bigelow EM, Jepsen, KJ. (2015) How Does Bone Strength Compare Across Sex, Site, and Ethnicity?, *Clin Orthop Relat Res* 473, 2540–2547.

Schilcher J, Michaëlsson K, Aspenberg P (2011) Bisphosphonate Use and Atypical Fractures Fractures of the Femoral Shaft', Bisphosphonate Use and Atypical Fractures of the Femoral Shaft, *Science* 364, 1728–1737.

Shane E, Burr D, Ebeling PR, et al. (2010) Atypical Subtrochanteric and Diaphyseal Femoral Fractures: Report of a Task Force of the American Society for Bone and Mineral Research, *J Bone Miner Res* 25, 2267–2294.

Shane E, Burr D, Abrahamsen B, et al. (2014) Atypical subtrochanteric and diaphyseal femoral fractures: Second report of a task force of the American society for bone and mineral research, *J Bone Miner Res* 29 1–23.

Shin WC, Moon NH, Jang JH, et al. (2017) Anterolateral femoral bowing and loss of thigh muscle are associated with occurrence of atypical femoral fracture: Effect of failed tension band mechanism in mid-thigh, *J Orthop Sci* 22, 99–104.

Smith RW Jr, Walker RR (1964) Femoral Expansion in Aging Women: Implications for Osteoporosis and Fractures, *Science* 145, 156–157.

Szolomayer LK, Ibe IK, Lindskog DM (2017) Bilateral atypical femur fractures without bisphosphonate exposure, *Skeletal Radiol*, 46, 241–247.

Taormina DP, Marcano AI, Karia R, et al. (2014) Symptomatic atypical femoral fractures are related to underlying hip geometry, *Bone* 63, 1–6.

Ward KA, Adams JE, Hangartner TN (2005) Recommendations for thresholds for cortical bone geometry and density measurement by peripheral quantitative computed tomography, *Calcif Tissue Int* 77, 275–280.

Figure and Table Legends

Figure 1: Method for calculating the threshold using the mode method

A histogram was created on the basis of a frequency table of CT values to calculate the mean CT value of the first peak (i.e., approximately -1,000; mainly indicating the CT value of the surrounding air) and the CT value of the second peak (i.e., indicating the CT value of the bone itself). An example of one slice is shown; CT image of the femoral diaphysis, width level (WL) 500 and windows width (WW) 2500. The calculated threshold value was 375, and the contour of the target bone was determined.

Figure 2: Methods to calculate each indicator

Left figure

Cortical bone thickness (CBT); distances between a point (a) on the periosteal surface and all points on the endosteal surface of the cortical bone were calculated. The minimum of these values was defined as the CBT of the point. Such calculations were performed for all points on the periosteal surface of the cortical bone to calculate the CBT of the entire circumference of the cortical bone.

Periosteal border length (PBL) of each section was calculated by counting the number of points (pixels) on the periosteal surface.

Right figure

The area of cross-section (ACS) of each section was calculated by counting all the points (pixels) in the area surrounded by the periosteal and endosteal perimeters of the cortical bone (b). The area was corrected by calculating the actual length per pixel in the DICOM data to take into account the magnification ratio at the time of imaging.

The ratio of the cortical bone area to the ACS of the femoral mid-diaphysis at Level 5 (i.e., the occupancy rate of the cortical bone) was calculated as the cortical index (CI_5; i.e., b / [b + c] × 100).

Figure 3: Analysis results from a 70-year-old female and a 60-year-old female

In this figure, the degree of CBT is visualized. The thicker the cortex, the deeper the red, whereas the thinner the cortex, the deeper the blue.

Figure 4: Analysis of results from a 70-year-old female and a 60-year-old female (same samples in Figure 3).

The shapes of the cross-sections for seven levels are shown. In the tables, the values of the mean cortical bone thickness (mCBT) (average ± standard deviation), periosteal border length (PBL), and area of cross-section (ACS) are shown. Progression of osteoporosis was observed in the 70-year-old female.

Figure 5: Cross-sectional images at Level 5 for each individual are shown in ascending order of cortical index at Level 5 (CI_5) values. Blue indicates images from males, and red indicates those from females. The number at the center of each figure indicates the age of the individual.

Figure 6: Values of the cortical index at Level 5 (CI_5)

6-a) Scatter plot showing the relationship between CI_5 and age in males and females

6-b) Box plots of CI_5 values according to age (i.e., group A, ≤69 years old and group B, ≥70 years old) and sex (** $p<0.01$).

Figure 7: Results of the measurement of cortical bone thickness (CBT)

7-a) Box plots of the comparison of group A (≤69 years old, 30 males and 16 females) and group B (≥70 years old, 16 males and 28 females) (* $p<0.05$, ** $p<0.01$).

7-b) Scatter plot showing the relationship between mCBT and age in males and females.

Figure 8: Results of area of cross-section (ACS) measurements

8-a) Box plots of ACS values at Levels 2–8 according to age (i.e., group A, ≤69 years old and group B, ≥70 years old) and sex (* $p<0.05$, ** $p<0.01$).

8-b) Scatter plot showing the relationship between ACS values and age in males and females.

Figure 9: Results of the periosteal border length (PBL) measurement

9-a) Box plots of PBL values at Levels 2–8 according to age (i.e., group A, ≤69 years old and group B, ≥70 years old) and sex (* $p<0.05$).

9-b) Scatter plot showing the relationship between mean PBL and age in males and females.

Table 1: Comparison between the level of the maximal mean cortical bone thickness (mCBT) and that of the maximal area of cross-section (ACS).

The level of the maximal ACS value and that of the maximal mCBT in each femoral bone is shown. The region with the largest ACS was located more proximal to the region with the largest mCBT in 48 of 90 individuals (asterisk).

Figure 1

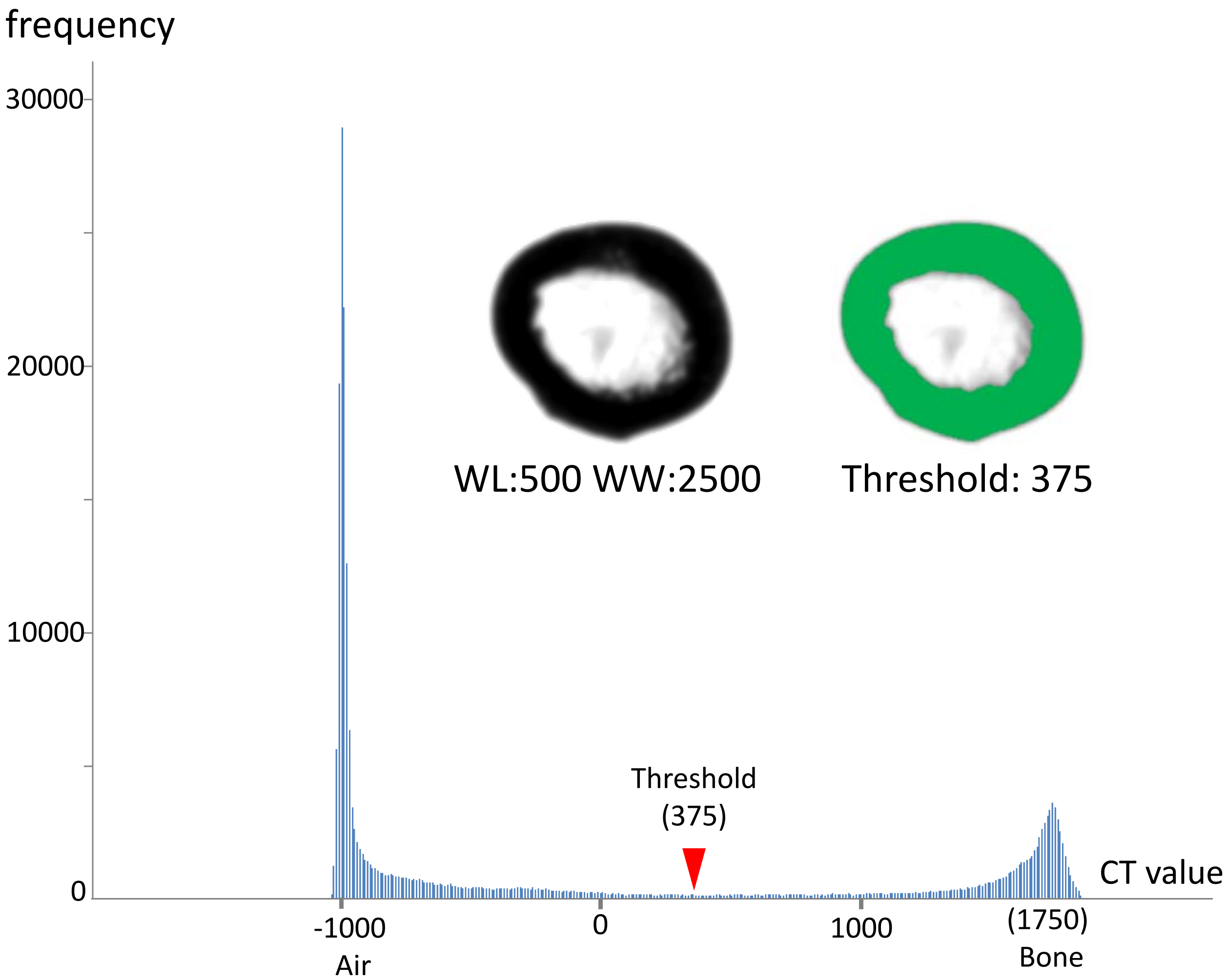
frequency
30000
20000
10000
0
WL:500 WW:2500
Threshold: 375
Threshold
(375)
CT value
-1000
Air
0
1000
(1750)
Bone

Figure 2

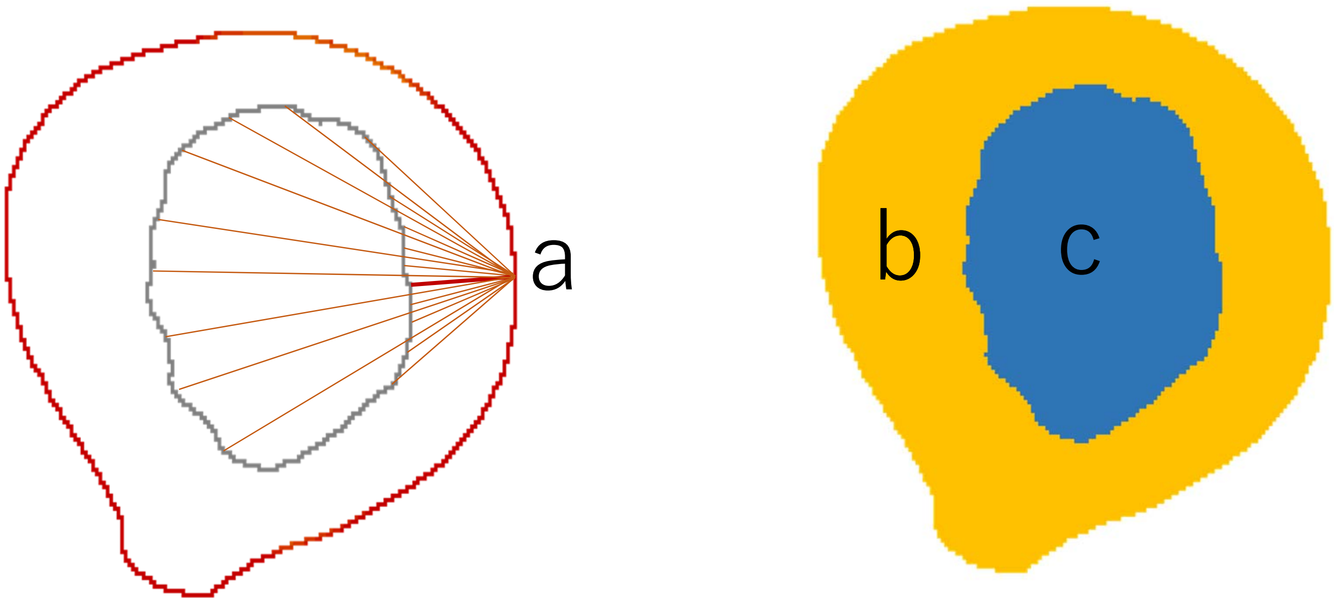

Figure 3

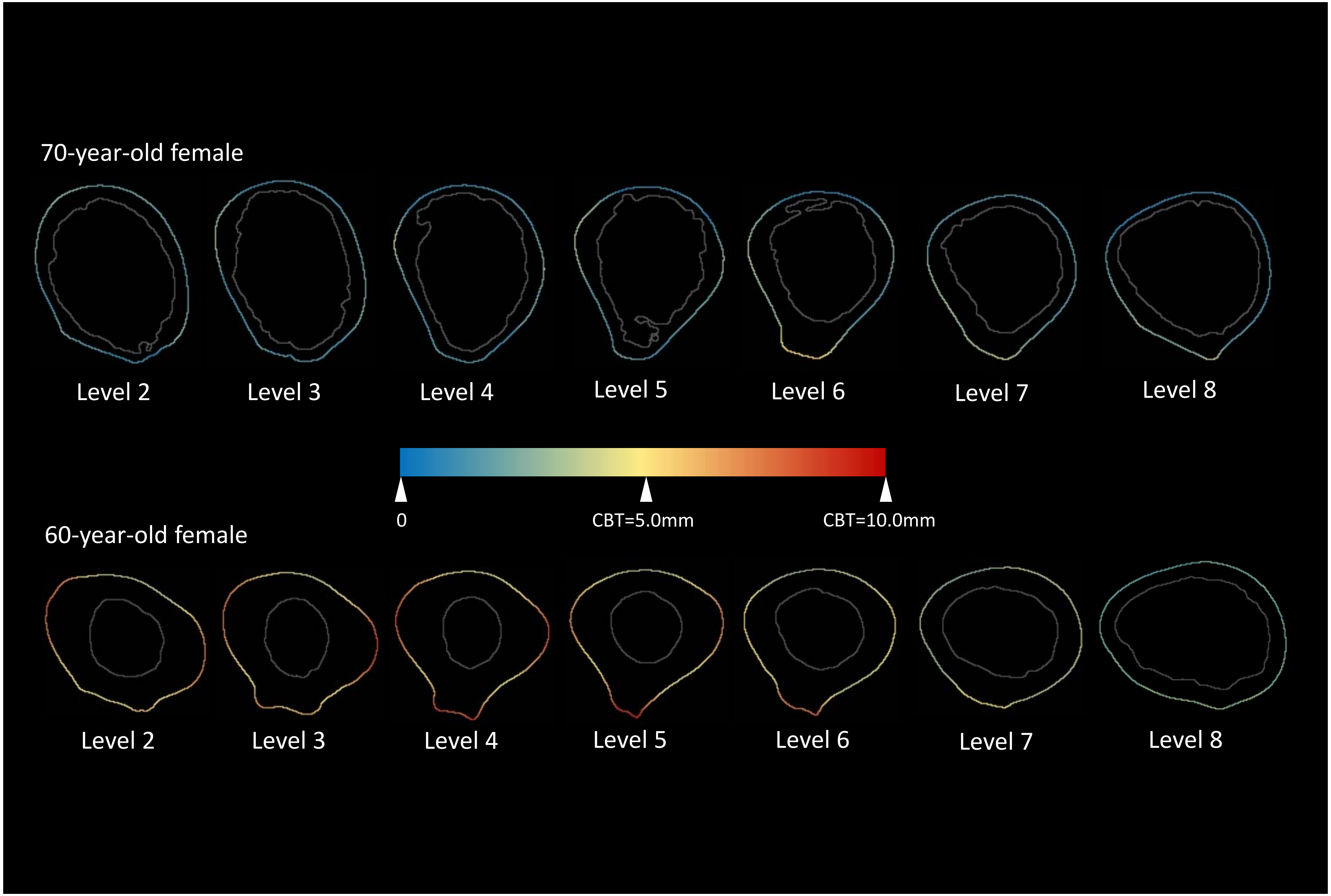
70-year-old female
Level 2
Level 3
Level 4
Level 5
Level 6
Level 7
Level 8
0
CBT=5.0mm
CBT=10.0mm
60-year-old female
Level 2
Level 3
Level 4
Level 5
Level 6
Level 7
Level 8

Figure 4

70-year-old female

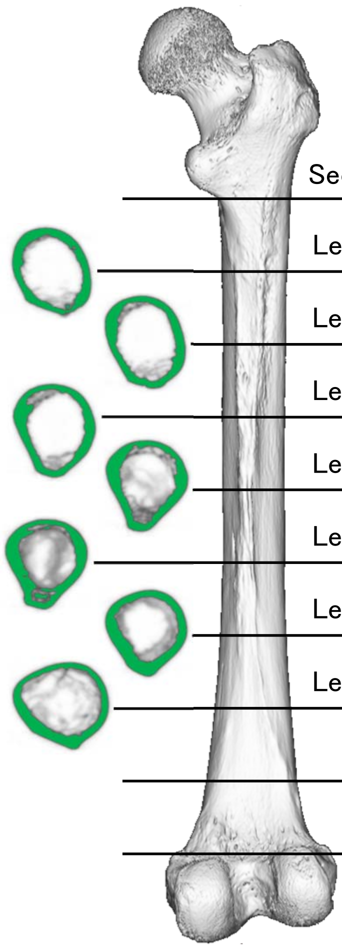

Section	mCBT* (mm)	PBL (mm)	ACS (mm^2)
Level 2	10.9± 2.7	100.0	172.1
Level 3	10.2± 2.8	100.3	163.9
Level 4	9.9± 3.2	99.2	157.2
Level 5	10.9± 3.7	97.0	168.6
Level 6	14.8± 7.1	94.4	192.4
Level 7	12.6± 4.0	94.4	171.5
Level 8	9.8± 3.8	100.0	150.2

60-year-old female

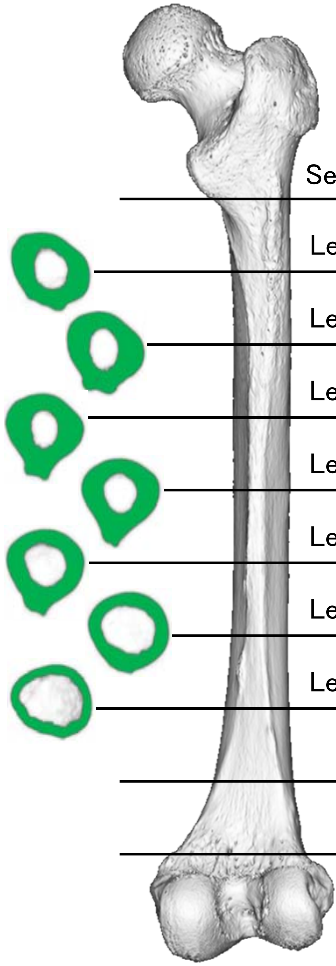

Section	mCBT* (mm)	PBL (mm)	ACS (mm^2)
Level 2	30.5± 6.6	101.7	349.7
Level 3	30.3± 6.5	101.7	364.1
Level 4	30.4± 7.1	103.6	362.5
Level 5	27.9± 7.3	103.2	336.5
Level 6	23.3± 6.0	101.7	311
Level 7	19.3± 3.4	103.6	278.8
Level 8	15.2± 1.8	114.0	248.7

Figure 5

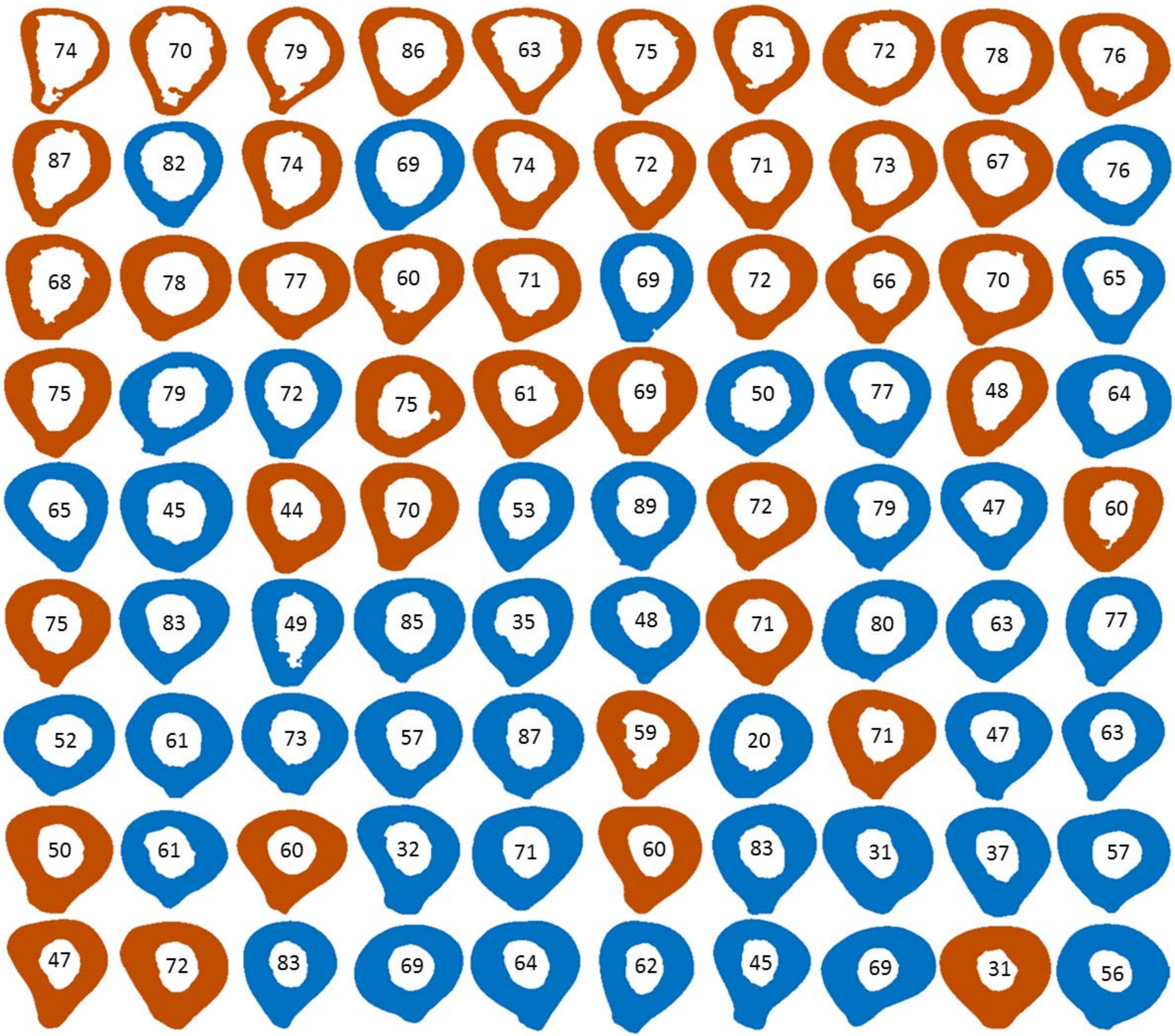

74 70 79 86 63 75 81 72 78 76
87 82 74 69 74 72 71 73 67 76
68 78 77 60 71 69 72 66 70 65
75 79 72 75 61 69 50 77 48 64
65 45 44 70 53 89 72 79 47 60
75 83 49 85 35 48 71 80 63 77
52 61 73 57 87 59 20 71 47 63
50 61 60 32 71 60 83 31 37 57
47 72 83 69 64 62 45 69 31 56

Figure 6

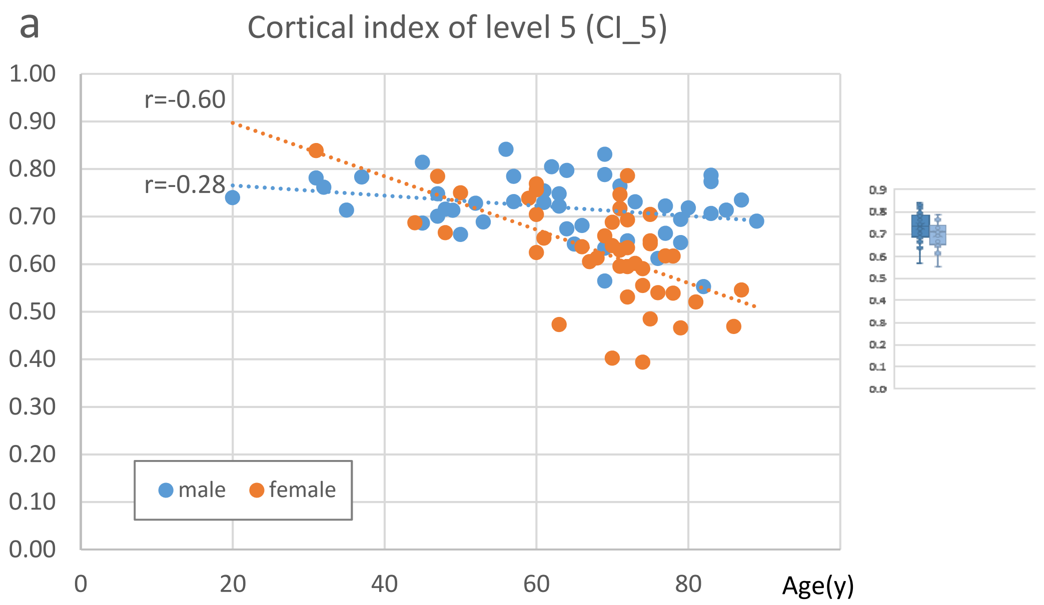

Figure 6-a

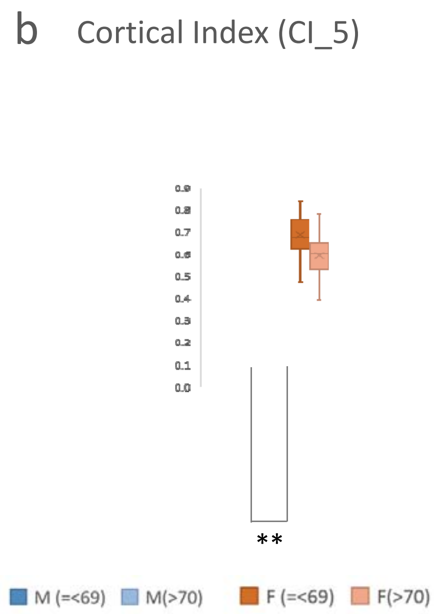

Figure 6-b

Figure 7

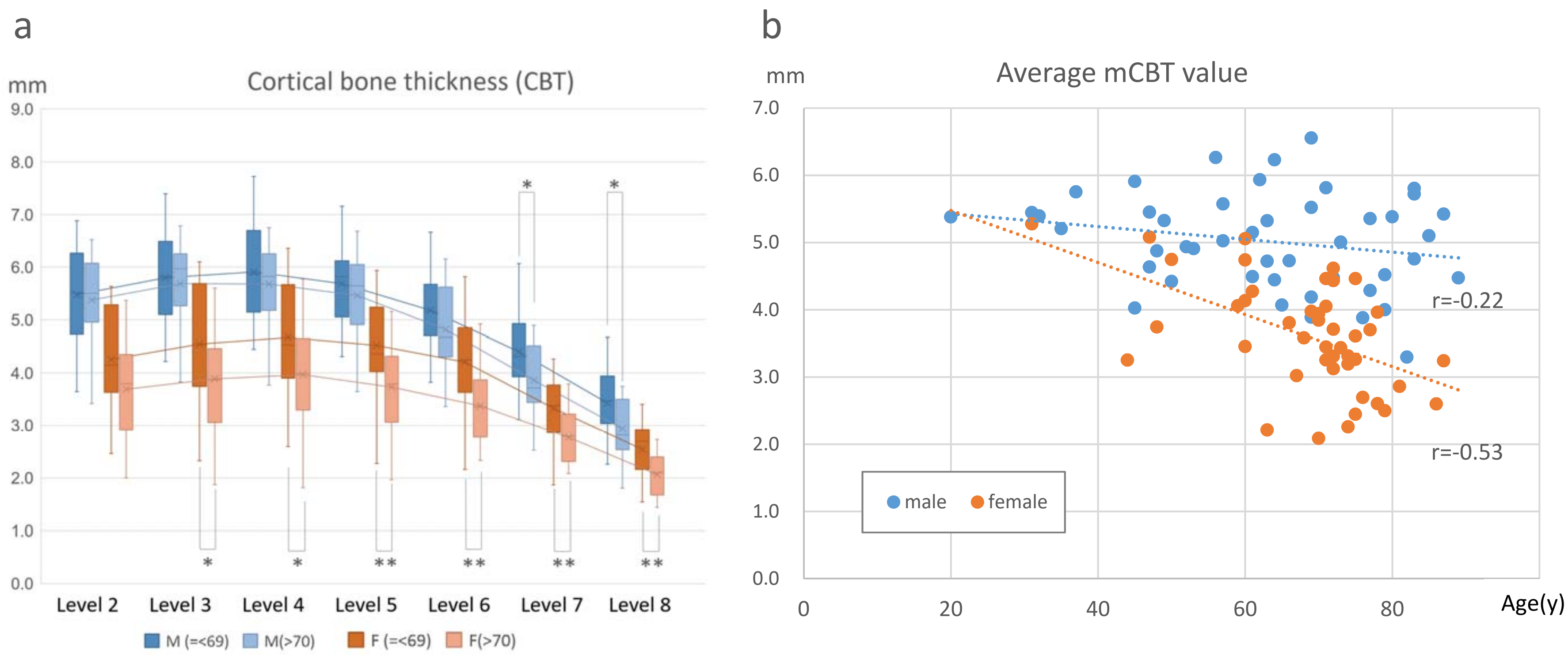

Figure 7-a

Figure 7-b

Figure 8

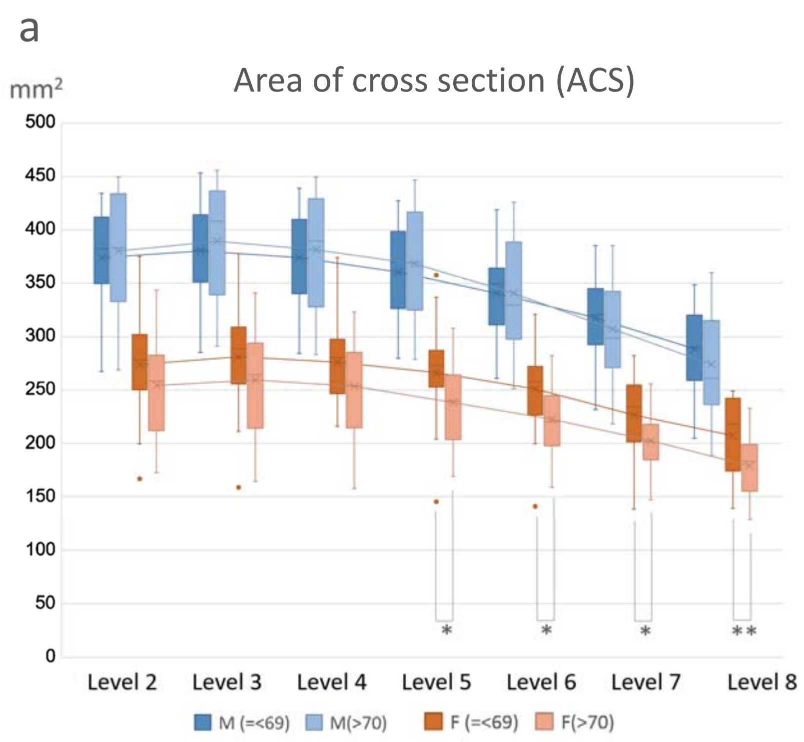

Figure 8-a

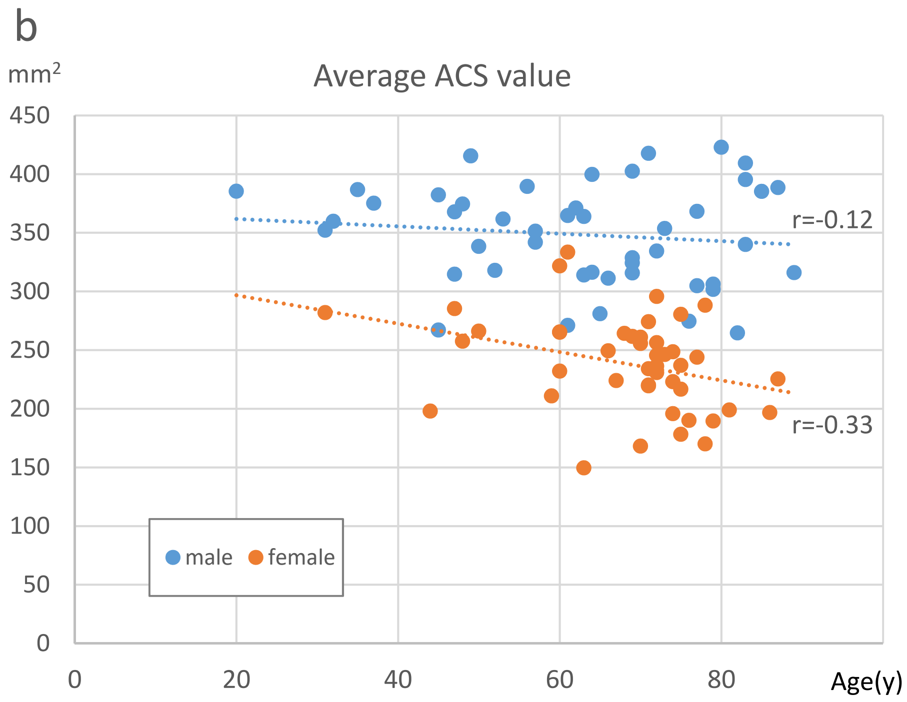

Figure 8-b

Figure 9

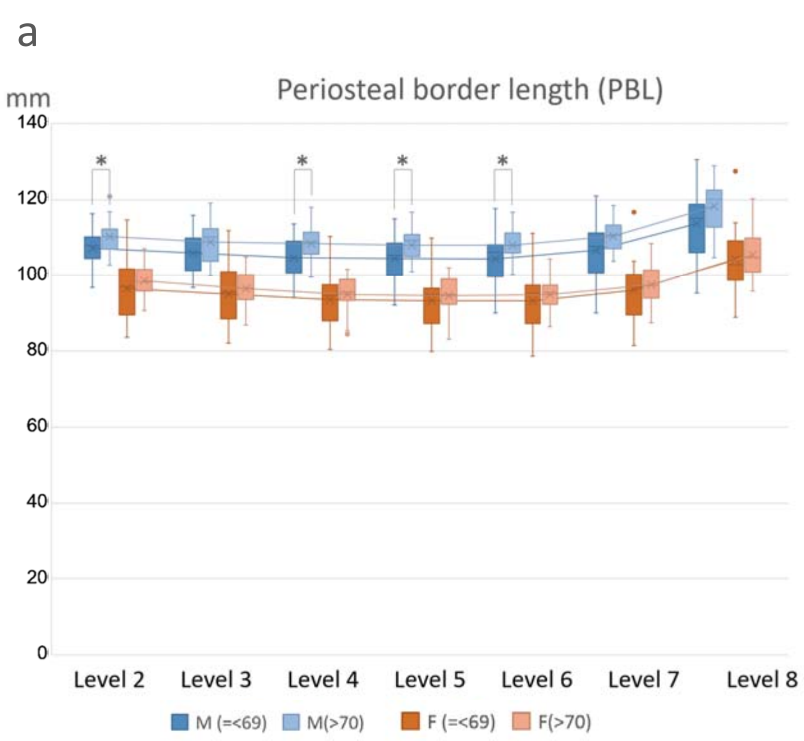

Figure 9-a

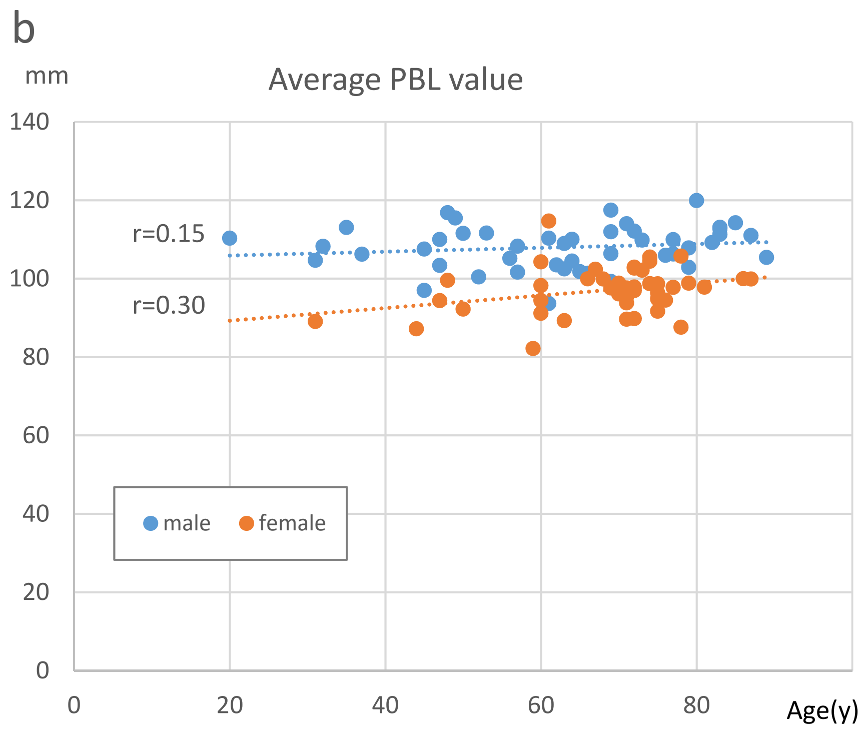

Figure 9-b

Table 1

		mCBT					
		Level 2	Level 3	Level 4	Level 5	Level 6	Total
ACS	Level 2	4	6*	7*	0	0	17
	Level 3	1	22	25*	7*	1*	56
	Level 4	0	0	7	2*	0	9
	Level 5	0	0	0	5	0	5
	Level 6	0	0	0	0	3	3
	Total	5	28	39	14	4	90